

Effect of Pipe Wall Roughness On Porous Breakwater Structure On Wave Deformation

A. M. Syamsuri ^{#1}, D. A. Suriamihardja ^{#2}, M. A. Thaha ^{#3} and T. Rachman ^{#4}

^{#1}Doctoral Student, Department of Civil Engineering, Faculty of Engineering, Hasanuddin University, Jalan Poros Malino, KM-6 Gowa, South Sulawesi, Indonesia.

^{#2}Department of Geophysics, Faculty of Sciences, Hasanuddin University, Jalan Perintis Kemerdekaan KM-10 Makassar, South Sulawesi, Indonesia.

^{#3}Department of Civil Engineering, Faculty of Engineering, Hasanuddin University, Jalan Poros Malino KM-6 Gowa, South Sulawesi, Indonesia.

^{#4}Department of Ocean Engineering, Faculty of Engineering, Hasanuddin University, Jalan Poros Malino KM-6 Gowa, South Sulawesi, Indonesia

¹syamsuriandimakbul@yahoo.co.id, ²dahmaduh@gmail.com, ³arsyad999@gmail.com

Abstract - Waves are raised on the flume and interact with porous breakwater structures. As a result of these interactions, waves will experience reflection, dissipation, and transmission. The research was conducted with a model of pipe wall roughness to analyze the reflection coefficient and high wave transmission coefficient on each change in the coefficient value of pipe wall roughness. The roughness of the pipe wall depends on the parameters of pipe diameter, pipe length, and water depth on a porous breakwater. The study was conducted with experimental laboratory methods using wave generation flume with three-period variations (T ; 1.0 seconds, T ; 1.1 seconds, T ; 1.2 seconds), and three variations in water depth ($d=1.0h$; $d=1.1h$ and $d=1.2h$) of which h is the height of the model. The results showed that the roughness of the pipe wall affected reflection waves and transmission waves. The greater the coefficient of the roughness of the pipe wall, the higher the wave height.

Keywords — roughness of pipe wall, wave reflection, wave transmission

I. INTRODUCTION

Breakwater is a coastal structure building used to anticipate and control abrasion, one of the alternative functions of keeping the coastline from waves or reducing wave energy. Recently, there has been a lot of research in developing effective wave retaining structures that can reduce wave energy and provide positive benefits. One of the wave damper structures that is now undergoing research development is the porous breakwater. In 1961 a porous breakwater was first proposed by Jarlan and then widely developed by other researchers of them [4] trying to reduce the wave force that hit the front of the breakwater.

One of the essential characteristics of porous breakwaters is that the wave energy will break when it hits the permeable and porous front wall; the coming wave will pass through the hole on the model will reduce the occurrence of wave reflection in front of the structure. Porous breakwater is expected to minimize wave reflection and reduce transmission waves due to its ability to absorb wave energy and reduce coming wave energy. If the wave

energy passes through a surface, then the wave energy will be reduced along with increasing surface roughness.

Porous breakwater is expected to dampen wave energy using pipe structure with wall roughness surface; model testing in this study is studying wave reflection and transmission changes due to different roughness of the pipe wall. Therefore, test models are necessary to compare differences and wave responses to various conditions in diameter and depth.

II. LITERATURE STUDY

On a beach with a mild slope, wave heights may be increased by the influence of the wave set-up. Permeable breakwaters are planned in several ports to keep sea-water exchange [11].

Breakwater is a structure to protect waters from wave interference. The design separates the port basin from the open sea so that sea waves will not enter the bay. In applying for deepwater conditions, the floating breakwater is more efficient than conventional types because it requires less material. Floating breakwater is suitable for soft soils where the strength of the soil is low and is also good for the environment. The development of floating breakwater has increased significantly in the past decade [8]. Numerical and physical models have been developed to study the nonlinear dynamic interaction between water waves and permeable submerged breakwater over a finite thickness sand seabed [9]. Besides, the mathematical model was used to investigate the wave transmission coefficients of three breakwaters. The nonlinear wave propagation behaviors and the energy transfer from lower frequencies to higher frequencies after the submerged breakwater were investigated in detail [10].

Essential parameters for explaining water waves are wavelengths, wavelenghts, and the depth of water they spread. Other parameters such as speed influence determined from the three primary parameters above. As for the understanding of some of the parameters above [6]: Wavelength (L) is the horizontal distance between two peaks or the highest point of consecutive waves; it can also stated as the distance between two wave valleys [12]. Wave period (T) is the time required by two consecutive wave peaks/valleys passing through a given point. Wave



speed (celerity) (C) is a comparison between wavelength and wavelength (L/T). When the water wave travels at the speed of C., water particles do not move in the direction of wave propagation. While the coordinate axis to explain the motion of the waves is at a depth of the calm water face. The amplitude (a) is the distance.

A. Wave Deformation

Wave deformation is a change like waves that occur when waves move to the coast; changes or commonly called deformation of such waves include refractive, diffraction, and reflection. When viewed from the depth of the water where the waves spread, the waves grouped into three categories: shallow-water waves, transitions, and deep water. The limitations of the three categories based on the ratio between depth and wavelength (d/L). Waves can also be grouped by the ratio between wave height and wavelength, in this grouping known as small-amplitude waves and infinite amplitude waves (Stock, Cnoidal, Solitair). Small amplitude waves with Airy wave theory are derived based on the assumption [7] that the comparison between wave height and length or depth is minimal.

In contrast, the theory of amplitude waves account for the magnitude. If a wave propagates through a barrier, it reflected by the barrier. If the corrector is perfect or the wave comes reflected entirely, then the wave height in front of the barrier becomes twice the height of the coming wave and is called the standing wave. However, if the barrier has porosity or cannot reflect perfectly, then the wave height in front of the barrier will be less than twice the height of the coming wave, and in this condition, it is called a partial (partial) standing wave. A partial wave event is a wave that hits the beach or breakwater undergoes an imperfect energy reflection.

If a wave that experiences imperfect reflection hits a barrier, then the wave height coming Hi will be greater than the wave height reflected Hr. The wave period comes, and the reflected is the same, so the wavelength is also the same. The total wave profile in front of the barrier is [1]:

$$\eta = \frac{H_i}{2} \cos(kx - \sigma) + \frac{H_r}{2} \cos(kx + \sigma + \varepsilon) \dots \dots \dots (1)$$

Due to imperfect reflection, there are no actual nodes of the wave profile. To separate the height of the coming wave and the reflected wave height, Equation (2) is written in other forms as follows:

$$\eta_t = \frac{H_i}{2} (\cos kx \cos \sigma + \sin kx \sin \sigma) + \frac{H_r}{2} (\cos(kx + \varepsilon) \cos \sigma - \sin(kx + \varepsilon) \sin \sigma) \dots \dots \dots (2)$$

$$\eta_r = \left(\frac{H_i}{2} \cos kx + \frac{H_r}{2} \cos(kx + \varepsilon) \right) \cos \sigma + \left(\frac{H_i}{2} \sin kx - \frac{H_r}{2} \sin(kx + \varepsilon) \right) \sin \sigma \dots \dots \dots (3)$$

By deciphering the equations (2) and (3), obtained maximum and minimum water level elevation for partial standing waves as follows [3]:

$$\eta_{t \max} = \frac{H_i + H_r}{2} \dots \dots \dots (4)$$

$$\eta_{t \min} = \frac{H_i - H_r}{2} \dots \dots \dots (5)$$

By eliminating Equations (4) and (5) obtained:

$$H_i = \frac{H_{\max} + H_{\min}}{2} \dots \dots \dots (6)$$

$$H_r = \frac{H_{\max} - H_{\min}}{2} \dots \dots \dots (7)$$

If the wave comes to hit the partially transmitted barrier, then even passing waves will experience the same thing as hitting the barrier. If a barrier blocks the transmitted wave, the ht transmission wave height calculated by the formula:

$$H_t = \frac{(H_{\max})_t + (H_{\min})_t}{2} \dots \dots \dots (8)$$

When the comparison between the height of the wave of reflection with the height of the wave comes is called the coefficient of reflection and given the symbol Kr, as well as the comparison between the height of the transmission wave with the height of the coming wave is called the coefficient of transmission and given the symbol Kt. While the coefficient of energy loss is given the symbol Kd, Equation (7) can be written:

$$K_r + K_t + K_d = 1 \dots \dots \dots (9)$$

with :

$$K_t = \frac{H_t}{H_i} = \text{Wave Transmission Coefficient} \dots \dots \dots (10)$$

$$K_r = \frac{H_r}{H_i} = \text{Wave Reflection Coefficient} \dots \dots \dots (11)$$

B. Moody Diagram

Moody diagram is handy to calculate the flow in a pipe, to calculate the friction value in a pipe with a diameter, length, and pipe size. The easiest way is to read through the moody diagram even without knowing roughness of the pipe [5].

The Darcy-Weisbach Equation can calculate the basic theory of Head loss (loss of energy) in pipes due to friction as below:

$$h = \frac{fLv^2}{D2g} \dots \dots \dots (12)$$

with:

- h** = Loss of Energy
- f** = Friction Factor
- L** = Pipe Length
- V** = Fluid's Velocity
- D** = Pipe Diameter
- g** = Gravitational Force

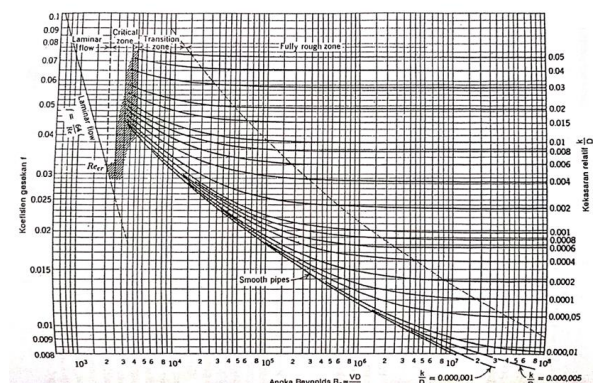


Figure 1. Moody Diagram

Moody's chart provides pipe friction factor, and this factor determined by Reynolds number and the relative roughness of the pipe. If the pipe gets rougher, then the

chances of turbulent will be greater. Relative roughness is defined as follows:

$$\frac{\epsilon}{D} \dots\dots\dots (13)$$

With :

ϵ = roughness

D = Pipe Diameter

while The Reynolds number defined as:

$$Re = \frac{Dv}{\zeta} \dots\dots\dots (14)$$

With :

Re = Reynold Number

D = Pipe Diameter

v = Velocity

ζ = viscosity kinematic fluid

Figure 1 of the moody diagram shows that the upper right corner is turbulent, and the top left is laminar. The relative roughness of the pipe stated on the right, then the Reynolds value at the bottom. Pull up until cutting the line, and then the value on the left side obtained the value of the coefficient of friction factor (f) and the type of turbulent flow or laminar.

III. METHODOLOGY

A. Type of The Research

The type of research used is experimental, where the condition of the pipe wall roughness of the breakwater model arranged in such a way that the pores/holes contained in the model facing the coming wave, width, height, and length of the breakwater model arranged based on the dimension of wave generator flume. This study uses two data sources, namely physical model data, namely data obtained directly from physical model simulations in the laboratory, and secondary data, namely data obtained from existing research literature through laboratory research and field research related to porous breakwater research.

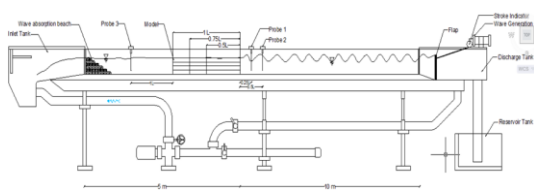


Figure 2. Models in wave generator flume

B. Parameters and Research Design

Pore/hole breakwater model, assembled pipe arrangement with Width (P) = ≥ 0.30 m (adjusted to flume width) and Model Height (h) = 0.29 m; 0.30 m. Model Length (B) = 0.50L; 0.75L; 1.0L; where L = 1.89 m (one wavelength), as well as pipes with roughness surface pipe wall diameter (D) is the range = ±0.145 m; ±0.097 m and ±0.075 m. Roughness material on the surface of the pore wall/pipe hole with four variations in roughness value that is without roughness (e0), rough sand (e1) diameter 0.3 - 0.5 cm; gravel (e2) diameter 0.7 - 0.9 cm, and coral (e3) diameter 1.0 - 1.2 cm, following Figure 3. visualization of

roughness on the surface of the pipe wall with some variations in the size of the granules as below



Figure 3. Variations in roughness on pipe wall surfaces

Data retrieved by measuring predetermined water depth (d) (adjusted flume height), i.e., d=1.2h (0.36 m); d=1.1h (0.32 m) and d=1.0h (0.29 m), then set the stroke distance on the flap to 3 stroke variations, i.e., 4, 5 and 6 and set the wave period variations, i.e., T1=1.0 seconds, T2=1.1 seconds and T3=1.2 seconds, where h is the model height, the model position on the wave channel must be at the correct placement so that it is effective when waves come or wave reflection in front of the model, as well as placing the position of probe1 and probe 2 in front of the wave direction model while probe 3 is behind the model, the distance between probes 1 and 2 adjusted to 1/2 L[2].



Figure 4. Model placement and position of probe 1, probe 2 and probe 3

IV. RESULTS AND DISCUSSION

A. Wave height analysis

In laboratory research, the first step to know is the determination of wave period (T) and water depth (d) as parameters in obtaining wavelength (L) and wave height (H) both analytically and measurement in wave generation flume. Data retrieval is the reading of the upper and lower threads in each different probe to obtain Hmax or Hmin, following the results of analysis of wave data calculation as representative of various variations of data retrieval experiments:

1. Wavelength (L)

Wavelength is a function of depth (d) and period (T); in this study, the wavelength obtained in 2 ways, namely the calculation and observation/measurement results directly on wave generation flume. Wavelength is calculated according to depth and period as follows: For depth (d) = 0.36 m with the period (T) = 1.2 seconds

$$L_0 = \frac{1,56 (T^2)}{d} = \frac{1,56 (1,2^2)}{0,36} = \frac{2,246}{0,36} = 6,239 \text{ m}$$

$$\frac{L_0}{L} = \frac{6,239}{L} = 0,1602 \text{ substitutes } \frac{d}{L} = 0,1917$$

Where $\frac{d}{L_0} = \frac{d}{L}$ (Function Table $\frac{d}{L}$ for Increasing $\frac{d}{L_0}$ value)

$$L = \frac{d}{d/L} = \frac{0,36}{0,1909} = 1,89 \text{ m}$$

2. Incoming Wave Height (H_i)

The incoming wave height (H_i) in flume wave generation occurs in front of the model, the value of H_i obtained from the division of H_{max} and H_{min} values contained in probe 1 and probe 2. Here are the results of the calculation of the coming wave height (H_i):

$$(H_i) = \frac{H_{max}(\text{probe2}) + H_{min}(\text{probe1})}{2}$$

$$H_{max}(\text{probe2}) = 3,9385_{(\text{probe2})} - (-2,9810)_{(\text{probe2})} = 6,8195 \text{ cm}$$

$$H_{min}(\text{probe1}) = 1,9117_{(\text{probe1})} - (-1,6658)_{(\text{probe1})} = 3,5775 \text{ cm}$$

$$(H_i) = \frac{6,8195 + 3,5775}{2} = 5,1985 \text{ cm}$$

3. Reflected Wave Height (H_r)

Reflected Wave Height (H_r) in wave generation flume occurs in front of the model, the H_r value that has been reduced obtained from the division of H_{max} and H_{min} values is found in probe 1 and probe 2. Here are the results of the calculation of wave height reflection (H_r):

$$(H_r) = \frac{H_{max}(\text{probe2}) - H_{min}(\text{probe1})}{2}$$

$$H_{max}(\text{probe2}) = 3,4073_{(\text{probe2})} - (-2,9146)_{(\text{probe2})} = 6,3219 \text{ cm}$$

$$H_{min}(\text{probe1}) = 1,4984_{(\text{probe1})} - (-1,8208)_{(\text{probe1})} = 3,3192 \text{ cm}$$

$$(H_r) = \frac{6,3219 - 3,3192}{2} = 1,5013 \text{ cm}$$

4. Transmission Wave Height (H_t)

While the transmission wave height (H_t) occurs behind the model, the H_t value is obtained from the division of the H_{max} and H_{min} values found on probe 3. The calculation results of the transmission wave height (H_t):

$$(H_t) = \frac{H_{max}(\text{probe3}) + H_{min}(\text{probe3})}{2}$$

$$H_{max}(\text{probe3}) = 0,4281 \text{ cm}$$

$$H_{min}(\text{probe3}) = (-0,6667) \text{ cm}$$

$$(H_t) = \frac{0,4281 + (-0,6667)}{2} = 1,0948 \text{ cm}$$

B. Effect of Frictional Roughness (f) on K_t ; K_r

The value of the Friction Coefficient (f) is determined based on the relative roughness (ϵ / D) and the Reynolds

number (Re), so that if the pipe has a specific size and flow velocity, then the energy loss due to friction calculated immediately. Relative roughness is the ratio between the pipe wall roughness value and the pipe diameter, one of the results of the relative roughness calculation and the Reynolds number for model (D7,5) in model B = 1.0L) as follows:

$$\frac{\epsilon}{D} = \frac{0,00012}{0,075} = 0,0016 \text{ (relative roughness value)}$$

As for the Reynolds number :

$$Re = \frac{Dv}{\zeta} = \frac{(0,75 \times 1,390)}{(1,3 \times 10^{-6})} = 80192,31$$

The Friction Coefficient (f) on K_t and K_r from the analysis above, shown in the graph below

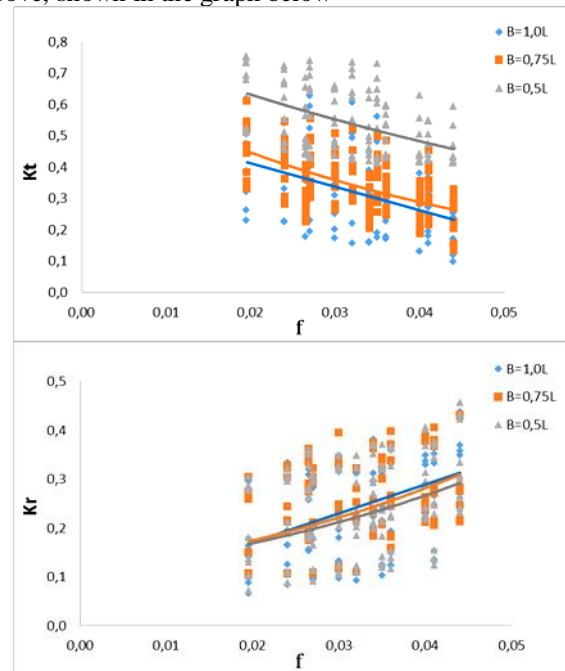


Figure 4. Relation of f vs K_t dan K_r on B=1,0L; B=0,75L and B=0,5L

The friction coefficient (f) to K_t in the three models shows that a significant decrease in the value of the transmission coefficient (K_t) as the increase in the value of friction coefficient (f) occurs in the three models when compared to the three models shows the value of K_t at B = 1.0L = 0.22 - 0.40; the K_t value at B = 0.75L = 0.24 - 0.42 and the K_t value at B0.5L = 0.45 - 0.61, this shows that in model B = 1.0L it is greater to reduce transmission waves than model B = 0.75L even though the interval difference is not too significant between the two. Still, in the B0.5L model, there is a very significant difference in the K_t value interval because the model B0.5L has the shortest dimension compared to other models so that the waves pass through the friction surface area are shorter than the other models so that the tendency of the waves to be passed is higher / bigger.

Meanwhile, the effect of the friction coefficient (f) on the reflection coefficient (K_r) has increased as the value (f)

increases. The greater the value of friction coefficient (f), the greater the value of K_r . Apart from that, the three models showed the same trend of increasing K_r value for each change in the different model parameters and had almost the same reflection coefficient value, where the K_r value at $B = 1.0L = 0.17 - 0.31$; the K_r value at $B = 0.75L = 0.17 - 0.30$ and the K_r value at $B = 0.5L = 0.17 - 0.28$, proving that the reflection wave has increased.

V. CONCLUSION

The research results show that the height of the transmission wave and the resulting reflection wave height are influenced by the pipe wall's roughness, the pipe diameter, and the length of the pipe. The greater the Friction Coefficient (f), the transmitted wave height decreases. In contrast, the resulting reflection wave height is inversely proportional to the more significant the Friction Coefficient (f), the resulting reflection wave increases.

References

- [1] Dean, R. G, Dalrymple (1984), *Water Waves Mechanics for Engineer and Scientist*. Prentice Hall, Inc., New Jersey; Englewood Cliffs.
- [2] Goda Y, Zusuki Y., 1976, Estimation of incident and reflected waves in random wave experiments. *Marine Hydrodynamics* Division Port and Harbour Research Institute, Ministry of Transport. Nagase, Yokosuka, Japan.
- [3] Paotonan, C (2006). *Unjuk Kerja Susunan Bambu Sebagai Pemecah Gelombang Terapung*. Tesis. Yogyakarta; Universitas Gadjah Mada.
- [4] Quin, A (1972). *Design and Construction of Ports and Marine Structures*. New York; McGraw Hill.
- [5] Triatmodjo, B (1993). *Hidraulika II*. Beta Offset, Yogyakarta.
- [6] Triatmodjo, B (1999). *Teknik Pantai*. Beta Offset, Yogyakarta.
- [7] Triatmodjo, B (2011). *Perencanaan Bangunan Pantai*. Beta Offset, Yogyakarta.
- [8] A B Widagdo et al 2020 *J. Phys.: Conf. Ser.* 1625 012055
- [9] Norimi Mizutani, Ayman M Mostafa, Koichiro Iwata, Nonlinear regular wave, submerged breakwater and seabed dynamic interaction, *Coastal Engineering*, Volume 33, Issues 2–3, 1998, Pages 177-202, ISSN 0378-3839, [https://doi.org/10.1016/S0378-3839\(98\)00008-8](https://doi.org/10.1016/S0378-3839(98)00008-8).
- [10] Yanxu Wang, Zegao Yin, Yong Liu, Ning Yu, Wei Zou, Numerical investigation on combined wave damping effect of pneumatic breakwater and submerged breakwater, *International Journal of Naval Architecture and Ocean Engineering*, 11(1)(2019) 314-328, ISSN 2092-6782, <https://doi.org/10.1016/j.ijnaoe.2018.06.006>.
- [11] Clark, C. A. (2011). An approach to computing acoustic wave propagation in shallow water. *The Journal of the Acoustical Society of America*, 130(4) 2529–2529. doi:10.1121/1.3655098
- [12] Fathy M. Mustafa, Saber H. Abd Elbaki, Tamer M. Barakat (2019). Performance of Backward Pumped Fiber Raman Amplifier with Different Fiber Types *International Journal of Engineering Trends and Technology*, 67(5) 79-84.